Volume 57
Number 37
7 May 2021
Pages 4473–4594

ChemComm

Chemical Communications

rsc.li/chemcomm

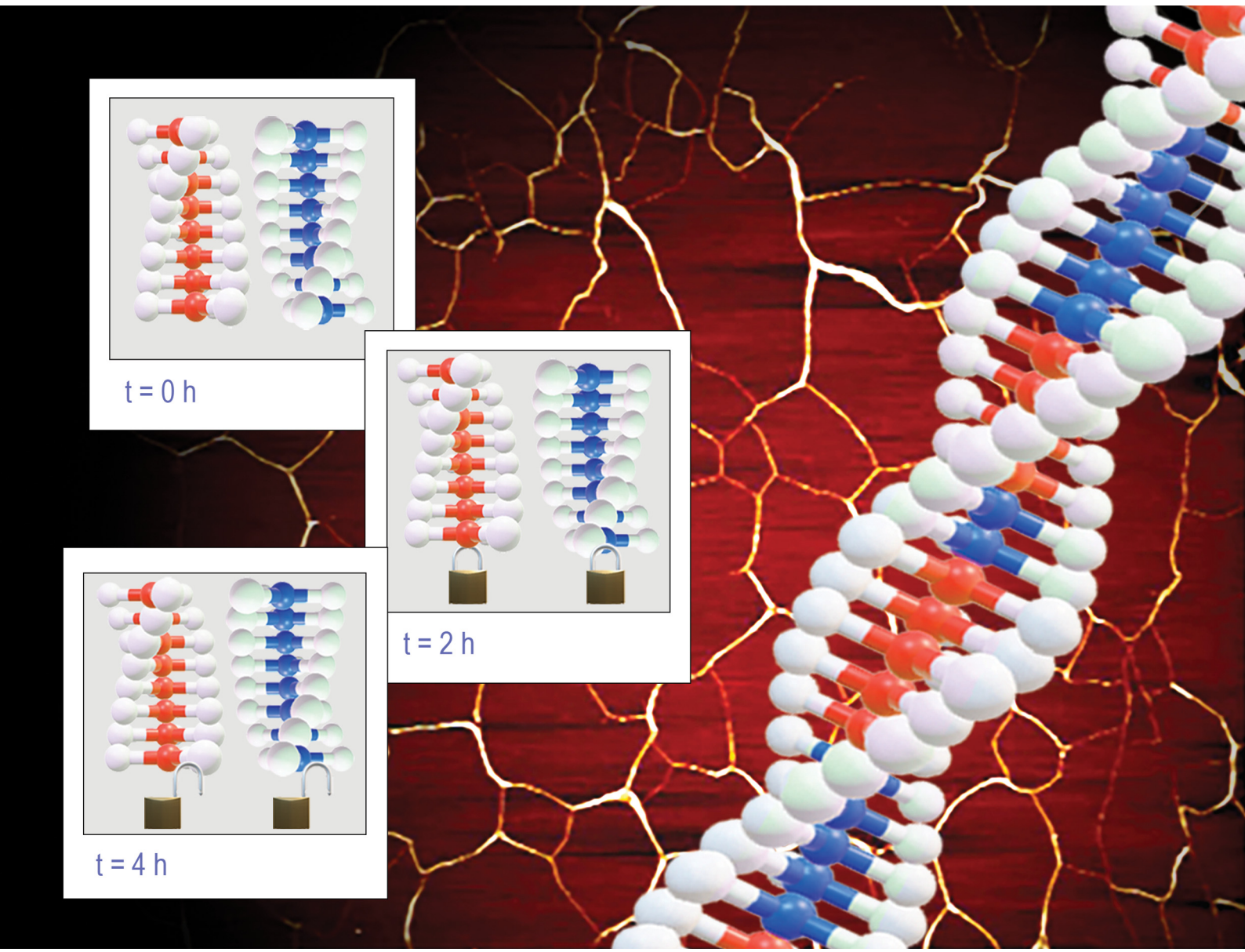

ISSN 1359-7345

ROYAL SOCIETY OF CHEMISTRY

COMMUNICATION

Gustavo Fernández, Luis Sánchez *et al.*

Chain-capper effect to bias the amplification of asymmetry in supramolecular polymers

ChemComm

COMMUNICATION

View Article Online
View Journal | View Issue

Cite this: *Chem. Commun.*, 2021, **57**, 4500

Received 8th February 2021,
Accepted 30th March 2021

DOI: 10.1039/d1cc00740h

rsc.li/chemcomm

Chain-capper effect to bias the amplification of asymmetry in supramolecular polymers†

Cristina Naranjo, [a] Yeray Dorca, [a] Goutam Ghosh, [b] Rafael Gómez,[a] Gustavo Fernández*[b] and Luis Sánchez *[a]

The kinetically controlled amplification of asymmetry experienced in the co-assembly of chiral tribiphenylaminetricarboxamides (*S*)-1 and (*R*)-1 is investigated. The formation of metastable monomeric species through intramolecular H-bonds retards the efficient amplification of asymmetry due to a chain-capper effect.

Amplification of asymmetry is the phenomenon by which enantioenriched entities are attained for the action of a chiral initiator.[1,2] This effect was extensively investigated by Green *et al.* in polyisocyanates that adopt enantioenriched, helical structures in Sergeants-and-Soldiers (SaS) or Majority Rules (MRs) experiments.[3] In the former, mixtures of achiral and chiral congeners are mixed and the final helical outcome is dictated by the chiral partner. In the latter, two different enantiomers of the same system are mixed at different ratio, the final helical sense being conditioned by the component added in excess.[2,3] Based on these studies, a number of examples on amplification of asymmetry has been described for supramolecular polymers.[4,5] Merocyanines,[6] naphthalene bisimides,[7] perylene bisimides,[8] or other π-conjugated systems[9] are scaffolds utilized to achieve helical supramolecular polymers. In addition, C_3-symmetric platforms represent archetypal examples to investigate the amplification of asymmetry in supramolecular polymers.[10–13] Importantly, the amplification of asymmetry in these systems has been primarily studied under thermodynamic control. Much less is known, however, about amplification of asymmetry under kinetic control. To the best of our knowledge, the kinetic traps formed by merocyanines,[6] carbonyl-bridged triarylamines,[14] and barbituric-based derivatives[15] have been demonstrated to yield different aggregates depending on the experimental conditions. Thus, the scarce number of molecular platforms exhibiting amplification of asymmetry under kinetic control makes necessary the development of new systems to gain further understanding of this phenomenon.

Herein, we report on the kinetically controlled amplification of asymmetry of C_3-symmetric trisbiphenylamine-tricarboxamides (***S*)-1** and (***R*)-1** (Fig. 1a). Unlike the previous report on these structures,[16] circular dichroism (CD) measurements reveal a cooperative supramolecular polymerization mechanism yielding only one type of aggregated species with fibrillar morphology. The flexible ethylene linker in (***S*)-1** and (***R*)-1** together with the presence of both benzamide and benzoester groups allow the formation of an intramolecularly H-bonded pseudocycle (Fig. 1a). The resulting metastable monomers (*M**) retard the amplification of asymmetry in the corresponding MRs experiments performed by mixing (***S*)-1** and (***R*)-1** due to a chain-capper effect by which the *M** species block temporally the growth of the columnar aggregates (Fig. 1c).[17] Thus, only 24 h

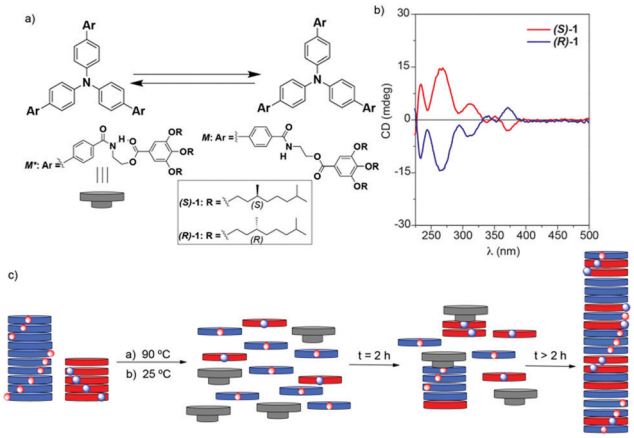

Fig. 1 (a) Chemical structures of the trisbiphenylamine-tricarboxamides (***S*)-1** and (***R*)-1** and the formation of the H-bonded pseudocycle; (b) CD spectra of (***S*)-1** and (***R*)-1** (MCH, c_T = 20 μM; 20 °C); (c) Schematic illustration of the chain-capper effect exerted by *M** in the MRs experiments.

[a] *Departamento de Química Orgánica, Facultad de Ciencias Químicas, Complutense de Madrid, Ciudad Universitaria, s/n, 28040, Madrid, Spain. E-mail: lusamar@ucm.es*

[b] *Organisch-Chemisches Institut, Westfälische Wilhelms-Universität Münster, Corrensstraße 36, 48149 Münster, Germany. E-mail: fernandg@uni-muenster.de*

† Electronic supplementary information (ESI) available: Experimental procedures, Spectroscopic characterization, and supplementary figures. See DOI: 10.1039/d1cc00740h

after preparing the mixture of both enantiomers, it is possible to achieve homochiral mixtures at values of the enantiomeric excess (ee) of ~0.30. These results contribute to shed light on the intricate processes related with chirality in supramolecular polymers.

The target compounds **(*S*)-1** and **(*R*)-1** have been prepared by following a modified procedure to that previously reported for **(*S*)-1** (see, ESI†).[16] In this case, tris(4-bromophenyl)amine was reacted with 4-methoxycarbonylphenylboronic acid in a Suzuki cross-coupling reaction, and the resulting triester was hydrolysed in basic medium to yield the corresponding tricarboxylic acid **4**.[18] A further reaction of **4** with the corresponding 2-aminoethyl 3,4,5-trialkoxybenzoate **(*S*)-** or **(*R*)-5**[19] yielded **(*S*)-1** or **(*R*)-1** in good yields (Scheme S1, ESI†). All the compounds were characterized by the habitual spectroscopic techniques (ESI†).

In our previous report, the supramolecular polymerization of **(*S*)-1** was investigated by UV-Vis measurements in methylcyclohexane (MCH), revealing an isodesmic mechanism.[4,16] This finding was highly unexpected since the vast majority of supramolecular polymers assembled by the synergy of H-bonding and π-stacking interactions, including the achiral congener of **(*S*)-1** and **(*R*)-1**,[16] are governed by a cooperative mechanism.[7–14] This is the case of **(*S*)-1** and **(*R*)-1** that self-assemble through H-bonding interactions between the amide functional groups and the π-stacking of the aromatic moieties, demonstrated by the corresponding variable-temperature (VT) and concentration ^{1}H NMR experiments (Fig. S1 and S2, ESI†).

The fibrillar nature of the aggregates formed by **(*S*)-1** and **(*R*)-1** in MCH, visualized by atomic force microscopy (AFM), constitutes an additional counterintuitive proof for the isodesmic mechanism tentatively elucidated for **(*S*)-1**. AFM images of MCH solutions of both **(*S*)-1** and **(*R*)-1** at a total concentration (c_T) of 10 μM show intertwined, long fibres of tenths of micrometers in length and typical heights of 4.5 nm (Fig. 2a, b, Fig. S3 and S4, ESI†), suggesting a cooperative mechanism. Compounds **(*S*)-1** and **(*R*)-1** form *M*- and *P*-type helical aggregates, respectively, as shows the corresponding dichroic pattern (Fig. 1b). Furthermore, the dichroic pattern observed for the aggregated species of **(*S*)-1** and **(*R*)-1** is very rich with maxima at λ = 233, 266, 315, 354, and 374 nm and isodichroic points at λ = 336, 357 and 388 nm. The CD response contrasts with the simple absorption pattern observed in the corresponding UV-Vis spectra (Fig. S5, ESI†) and prompted us to reinvestigate the supramolecular polymerization mechanism of these chiral units in more detail. Interestingly, registering the variation of the dichroic response by decreasing the temperature of diluted solutions of **(*S*)-1** and **(*R*)-1** revealed non-sigmoidal cooling curves that can be fitted to a cooperative mechanism by applying the one-component equilibrium (EQ) model.[20] This fitting shed values for the enthalpy of elongation, ΔH_e and the nucleation penalty, ΔH_n, of ~−150 and ~−15 kJ mol^{-1}, respectively. The derived value of the entropy of elongation (ΔS) is ~−400 JK mol^{-1} (Fig. 2c and Fig. S6 and Table S1, ESI†). The formation of kinetic traps resulting in a more complex supramolecular polymerization could account for the discrepancy between the UV-Vis and CD measurements and also for the appearance of unconventional amplification of asymmetry processes.[14b,16]

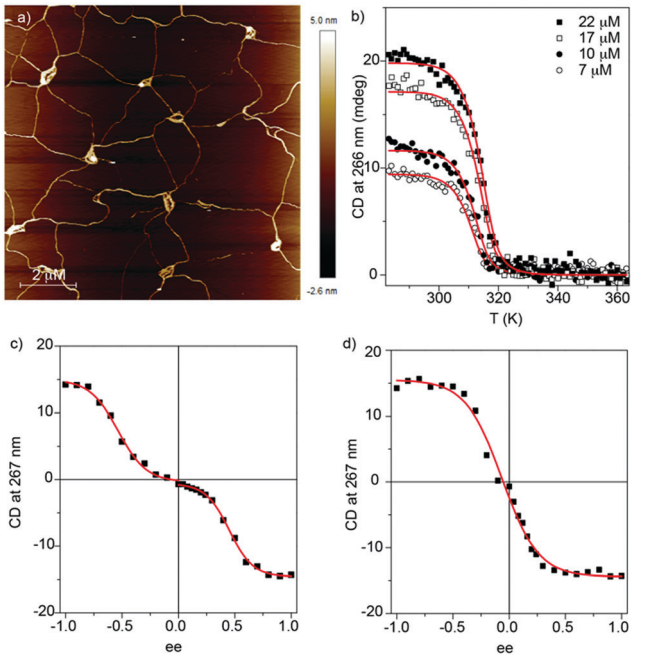

Fig. 2 (a) Height AFM image of the fibrillar aggregates of **(*R*)-1** in MCH spin-coated onto mica as surface (c_T = 10 μM); (b) Plot of the variation of the dichroic signal of **(*S*)-1** at λ = 266 nm *versus* temperature, cooling at 1 K min^{-1}. Red curves correspond to the fit to the EQ model. (c and d) Changes in CD intensity at λ = 267 nm as a function of ee upon mixing **(*S*)-1** and **(*R*)-1** at different ratios (MCH, 293 K, c_T = 20 μM) upon heating and cooling the mixture (a) and upon 24 h (b). The red curves correspond to a sigmoidal fit for guiding the eye.

After deriving the thermodynamic parameters, we have performed MRs experiments by mixing unequal amounts of **(*S*)-1** and **(*R*)-1** and keeping constant c_T at 20 μM. Prior to measure the CD spectra of the corresponding mixtures, we heated them up at 363 K and subsequently cooled them down to 293 K at a cooling rate of 1 K min^{-1}. Finally, the sample was equilibrated at 293 K for 10 min. In these conditions, amplification of asymmetry is attained only at large ees (~65%) (Fig. 3a and Fig. S7a, ESI†).

To further investigate this effect, we have firstly registered the kinetic evolution of the CD response. Thus, upon four hours, the dichroic response experiences no changes, which suggests the system is already under thermodynamic control (Fig. S8, ESI†). Thus, aging the samples for 24 h at 293 K drastically changes the amplification of asymmetry and a clear non-linear variation of the dichroic response is observed even at low ees, diagnostic of the achievement of a complete homochiral mixture at ee values of ~30% (Fig. 3b and Fig. S7b, ESI†). This variation has been fitted to the two-component EQ model to derive a mismatch penalty (MMP), the parameter that quantifies the penalty experienced by the incorporation of an enantiomer into a columnar aggregate of its unpreferred helicity.[20] A MMP value of −1.2 kJ mol^{-1} has been obtained (Table S1 and Fig. S9, ESI†).

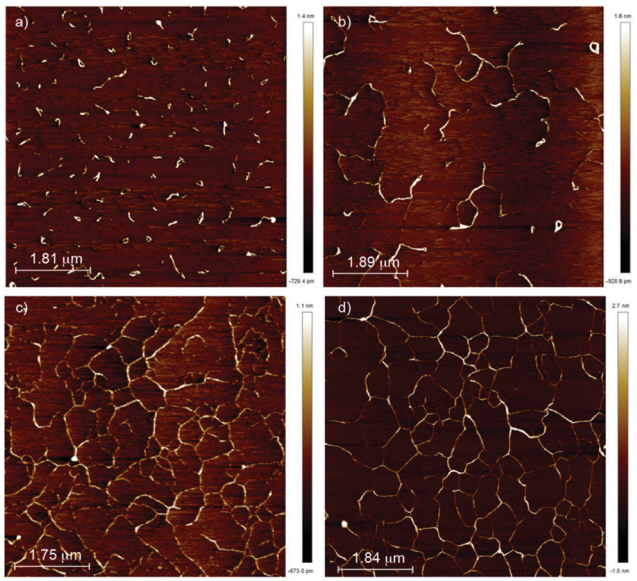

Fig. 3 AFM images of a mixture of **(*S*)-1** and **(*R*)-1** at ee = 0.4 after 15 min (a); 2 h (b), 4 h (c) and 24 h (d) upon preparing the mixture (MCH, c_T = 20 µM; 298 K).

To rationalize the kinetic effect observed in the MR experiments, it is important to consider the chemical structure of **(*S*)-1** and **(*R*)-1**. These tricarboxamides are endowed with both benzamide and benzoester units linked by an ethylene spacer. This molecular design allows the formation of an intramolecularly H-bonded seven-membered pseudocycle which is responsible for the appearance of a metastable monomeric species *M** (Fig. 1a).[14,20] The *M** species has been detected by using different spectroscopic techniques. Firstly, we have registered VT-^{1}H NMR experiments in $CDCl_3$ at c_T = 1 mM. These spectra show no shift for all the aromatic resonances, but the slight upfield shift of the triplet corresponding to the amide protons upon increasing the temperature is diagnostic of the rupture of the intramolecularly H-bonded pseudocycle (Fig. 1a and Fig. S10, ESI†).[20b] A definitive proof for the formation of *M** species has been attained by registering FTIR spectra in solution. Thus, in MCH, the N–H and Amide I stretching bands are observed at 3303 and 3304 and 1637 cm^{-1} for **(*S*)-1** and **(*R*)-1**, respectively, indicative of the formation of intermolecular H-bonding interactions between the amide functional groups (Fig. S11, ESI†). In chloroform, two bands ascribable to the N–H stretching are observed at 3460 and 3406 cm^{-1}. The former corresponds to free N–H amides whilst the latter, together with the Amide I band that appears at 1663 cm^{-1}, are accounted for the formation of the metastable monomeric species *M**.[21b,22]

Some reports on supramolecular polymers describe the participation of *M** species in pathway complexity.[21–23] We have utilized common techniques to probe the formation of different aggregated species [(1) thermal quenching; (2) slow cooling, (3) registering heating and cooling curves and (4) solvophobic quenching] with negative results.[24] Thus, the CD spectrum registered upon quenching a warm solution of **(*R*)-1** into an ice bath coincides with that registered for the solution upon cooling at 1 K min^{-1} (Fig. S12a, ESI†). Decreasing the cooling rate to 0.2 K min^{-1} displays similar UV-Vis or CD cooling curves than those attained by cooling at 1 K min^{-1} (Fig. S12b and S12c, ESI†). Finally, registering cooling and heating curves shows no hysteresis (Fig. S12b and c, ESI†). All these experimental results suggest that the *M** species do not efficiently interact with the species in their active conformation, in which the intramolecular H-bonding interaction is not operative. In this scenario, we have investigated the kinetic evolution of the formation of fibrillar structures in a mixture of **(*S*)-1** and **(*R*)-1** at ee = 0.4 and c_T =20 µM by AFM. After 15 min of preparing the mixture following the above mentioned procedure, only very short aggregates are observed. Upon aging the mixture for two hours, the length of the fibers grows until reaching a similar appearance than those visualized for the homopolymers after four hours. Aging the mixture for 24 h results in no morphological changes since the system is already under thermodynamic control (Fig. 1c, 3 and Fig. S13, ESI†). These AFM images indicate that the *M** species can act as kinetic chain-cappers that impede the further growing of the supramolecular homopolymers. The evolution of these dormant species allows a more efficient co-assembly of both enantiomers to afford homochiral aggregates.

Finally, and considering the MR experiments as an example of supramolecular copolymerization,[25] we have utilized the copolymerization model and the thermodynamic parameters collected in Table S1 (ESI†) to further investigate the co-assembly of **(*S*)-1** and **(*R*)-1**.[20b] The speciation plot shown in Fig. 4a displays the evolution of the concentration of both *M*- and *P*-type helical aggregates formed by **(*S*)-1** and **(*R*)-1** in the MR experiment, **(*S*)-1** being the major component. The predicted ee = 0.33, coincident with the experimental findings, is critical for observing drastic changes in the concentration of all the involved species in the MR experiment. Both *M*- and *P*-type helical supramolecular polymers formed by **(*S*)-1** and **(*R*)-1** grow until reaching an ee value of 0.33. At this point, an abrupt drop of all the helical species, except those formed by

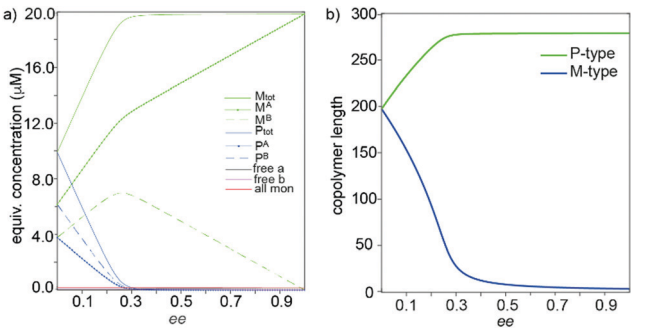

Fig. 4 Simulation of the copolymerization of **(*S*)-1** and **(*R*)-1** in the MR experiment (MCH, c_T = 20 µM, 293 K) showing (a) the equivalent polymer and monomer concentrations and (b) the copolymer length. Legend in Fig. 3a: free *a* = **(*S*)-1** monomers; free *b* = **(*R*)-1** monomers; *A* = supramolecular polymer formed by **(*S*)-1** and *B* = supramolecular polymer formed by **(*R*)-1**; *M* and *P* indicate the handedness of the helical supramolecular polymer.

the enantiomer present in excess (that rapidly grows until reaching an equivalent concentration of 20 μM), is observed (Fig. 4a). This effect is also predicted for the length of the aggregates, that undergoes a severe drop for the copolymer exhibiting the helicity of the minor enantiomer, and a strong growth for the copolymer with the handedness of the major enantiomer (Fig. 4b) (see ESI†).

In summary, we have reported the kinetically controlled amplification of asymmetry experienced by chiral trisbiphenylamine-tricarboxamides (***S***)-**1** and (***R***)-**1**. The intramolecularly H-bonded monomeric species retards, through a chain-capper effect, the efficient amplification of asymmetry that results in homochiral mixtures upon 24 h. The simulation of the MR process reveals the variation of the concentration of the different monomeric and supramolecular helical entities at a calculated value of ee = 0.33 that matches with the experimental value. The results presented herein demonstrate the potential that the synergy of experimental and theoretical models possesses to investigate and clarify complex processes like amplification of asymmetry in supramolecular polymers.

Financial support by the MCIU of Spain (CTQ2017-82706-P and RED2018-102331-T) and the Comunidad de Madrid (S2018/NMT-4389) is acknowledged.

Conflicts of interest

There are no conflicts to declare.

Notes and references

1 A. R. A. Palmans, E. W. Meijer and S. E. Denmark, *J. Polym. Sci.*, 2021, DOI: 10.1002/pol.20200814.
2 (*a*) A. R. A. Palmans and E. W. Meijer, *Angew. Chem., Int. Ed.*, 2007, **46**, 8948; (*b*) Y. Dorca, E. E. Greciano, J. S. Valera, R. Gómez and L. Sánchez, *Chem. – Eur. J.*, 2019, **25**, 5848.
3 (*a*) M. M. Green, M. P. Reidy, R. J. Johnson, G. Darling, D. J. O'leary and G. Willson, *J. Am. Chem. Soc.*, 1989, **111**, 6452; (*b*) M. M. Green, B. A. Garetz, B. Muñoz, H. Chang, S. Hoke and R. G. Cooks, *J. Am. Chem. Soc.*, 1995, **117**, 4181.
4 T. F. A. de Greef, M. M. J. Smulders, M. Wolffs, A. P. H. J. Schenning, R. P. Sijbesma and E. W. Meijer, *Chem. Rev.*, 2009, **109**, 5687.
5 L. Albertazzi, D. van der Zwaag, C. M. A. Leenders, R. Fitzner, R. W. van der Hofstad and E. W. Meijer, *Science*, 2014, **344**, 491.
6 A. Lohr and F. Werthner, *Angew. Chem., Int. Ed.*, 2008, **47**, 1232.
7 G. Ghosh, M. Paul, T. Sakurai, W. Matsuda, S. Seki and S. Ghosh, *Chem. – Eur. J.*, 2018, **24**, 1938.
8 (*a*) T. Kaiser, V. Stepanenko and F. Werthner, *J. Am. Chem. Soc.*, 2009, **131**, 6719; (*b*) T. Seki, A. Asano, S. Seki, Y. Kikkawa, H. Murayama, T. Karatsu, A. Kitamura and S. Yagai, *Chem. – Eur. J.*, 2011, **17**, 3598.
9 (*a*) A. Ajayaghosh, R. Varghese, S. J. George and C. Vijayakumar, *Angew. Chem., Int. Ed.*, 2006, **45**, 1141; (*b*) C. Kulkarni, R. Munirathinam and S. J. George, *Chem. – Eur. J.*, 2013, **19**, 11270; (*c*) F. Aparicio, B. Nieto-Ortega, F. Nájera, F. J. Ramírez, J. T. López Navarrete, J. Casado and L. Sánchez, *Angew. Chem., Int. Ed.*, 2014, **53**, 1373; (*d*) S. C. Karunakaran, B. J. Cafferty, A. Weigert-Muñoz, G. B. Schuster and N. V. Hud, *Angew. Chem., Int. Ed.*, 2019, **58**, 1453.
10 Y. Dorca, J. Matern, G. Fernández and L. Sánchez, *Isr. J. Chem.*, 2019, **59**, 869.
11 (*a*) M. M. J. Smulders, I. A. W. Filot, J. M. A. Leenders, P. van der Schoot, A. R. A. Palmans, A. P. H. J. Schenning and E. W. Meijer, *J. Am. Chem. Soc.*, 2010, **132**, 611; (*b*) M. M. J. Smulders, P. J. M. Stals, T. Mes, T. F. E. Paffen, A. P. H. J. Schenning, A. R. A. Palmans and E. W. Meijer, *J. Am. Chem. Soc.*, 2010, **132**, 620.
12 (*a*) F. García, P. A. Korevaar, A. Verlee, E. W. Meijer, A. R. A. Palmans and L. Sánchez, *Chem. Commun.*, 2013, **49**, 8674; (*b*) E. E. Greciano, J. Calbo, J. Buendía, J. Cerdá, J. Aragó, E. Ortí and L. Sánchez, *J. Am. Chem. Soc.*, 2019, **141**, 7463.
13 (*a*) S. Díaz-Cabrera, Y. Dorca, J. Calbo, J. Aragó, R. Gómez, E. Ortí and L. Sánchez, *Chem. – Eur. J.*, 2018, **24**, 2826; (*b*) Y. Dorca, R. Sánchez-Naya, J. Cerdá, J. Calbo, J. Aragó, R. Gómez, E. Ortí and L. Sánchez, *Chem. – Eur. J.*, 2020, **26**, 14700.
14 (*a*) J. S. Valera, R. Gómez and L. Sánchez, *Small*, 2018, **14**, 1702437; (*b*) J. S. Valera, R. Gómez and L. Sánchez, *Angew. Chem., Int. Ed.*, 2019, **58**, 510.
15 K. Aratsu, R. Takeya, B. R. Pauw, M. J. Hollamby, Y. Kitamoto, N. Shimizu, H. Takagi, R. Haruki, S. I. Adachi and S. Yagai, *Nat. Commun.*, 2020, **11**, 1623.
16 Y. Dorca, C. Naranjo, G. Ghosh, R. Gómez, G. Fernández and L. Sánchez, *Org. Mater.*, 2020, **2**, 41.
17 G. M. ter Huurne, P. Chidchob, A. Long, A. Martinez, A. R. A. Palmans and G. Vantomme, *Chem. – Eur. J.*, 2020, **26**, 9964–9970.
18 Y. Zhang, Y.-Q. Feng, J.-H. Wang, G. Han, M.-Y. Li, Y. Xia and Z.-D. Feng, *RSC Adv.*, 2017, **7**, 35672.
19 E. E. Greciano, B. Matarranz and L. Sánchez, *Angew. Chem., Int. Ed.*, 2018, **57**, 4697.
20 (*a*) H. M. M. ten Eikelder, A. J. Markvoort, T. F. A. de Greef and P. A. J. Hilbers, *J. Phys. Chem. B*, 2012, **116**, 5291; (*b*) H. M. M. ten Eikelder, B. Adelizzi, A. R. A. Palmans and A. J. Markvoort, *J. Phys. Chem. B*, 2019, **123**, 6627.
21 (*a*) S. Ogi, V. Stepanenko, K. Sugiyasu, M. Takeuchi and F. Würthner, *J. Am. Chem. Soc.*, 2015, **137**, 3300; (*b*) E. E. Greciano, S. Alsina, G. Ghosh, G. Fernández and L. Sánchez, *Small Methods*, 2020, **4**, 1900715.
22 M. Wehner, M. I. S. Röhr, M. Bühler, V. Stepanenko, W. Wagner and F. Würthner, *J. Am. Chem. Soc.*, 2019, **141**, 6092.
23 (*a*) E. E. Greciano, J. Calbo, E. Ortí and L. Sánchez, *Angew. Chem., Int. Ed.*, 2020, **59**, 17517; (*b*) J. Matern, Y. Dorca, L. Sánchez and G. Fernández, *Angew. Chem., Int. Ed.*, 2019, **58**, 16730.
24 (*a*) A. Sorrenti, J. Leira-Iglesias, A. J. Markvoort, T. F. A. De Greef and T. M. Hermans, *Chem. Soc. Rev.*, 2017, **46**, 5476; (*b*) J. Matern, K. K. Kartha, L. Sánchez and G. Fernández, *Chem. Sci.*, 2020, **11**, 6780.
25 B. Adelizzi, N. J. Van Zee, L. N. De Windt, A. R. A. Palmans and E. W. Meijer, *J. Am. Chem. Soc.*, 2019, **141**, 6110.